International Journal Of Renewable Energy Research, IJRER
J.Dayou, C.Man-Sang, Vol.1, No4, pp.323-332 ,2011

Performance Study of Piezoelectric Energy Harvesting to Flash A LED

Jedol Dayou*‡, Man-Sang, C.

* Energy, Vibration and Sound Research Group (e-VIBS), School of Science and Technology, Universiti Malaysia Sabah, Jalan UMS, 88400 Kota Kinabalu, Sabah, Malaysia

‡ Jedol Dayou : jed@ums.edu.my

Received:17.06.2011 Accepted:17.08.2011

Abstract- In this paper, analytical model of parallel and series configurations of identical piezoelectric benders with the increasing number is derived and studied to understand the performance of harvesting electric charge and power to flash a Light Emitting Diode (LED). Experiment was carried out where the flashing intervals of the LED were used to measure the harvesting performance. The benders in parallel configuration were found to perform the best as the number increases. The workability of the benders as a module of self-powered decorative LED as well as an autonomous sensor for monitoring shaking amplitude with reference to the flashing interval was then validated within the consideration of the structural damping.

Keywords- Ambient Vibration; Charge generation; Power harvesting; Piezoelectric bender; LED flashing.

1. Introduction

Mechanical vibration is a potential energy source that is abundant enough to be acquired from surroundings. It can be converted into electrical energy through piezoelectric transducer. As a result, this opens the possibility for developing an autonomous system and the need to power this system has motivated many research efforts focused on harvesting electrical energy from ambient vibration. These included the previous work at the MIT Media Lab to investigate the feasibility of harnessing energy parasitically from various human activities [1]. The work was later extended to study using piezoelectric ceramics for the collecting energy by walking [2]. More recently the piezoelectric element has been used simultaneously as a power generator and a sensor [3-8]. They have evaluated the performance of the piezoelectric sensor to power wireless transmission (most of them are RF transmission) and validated the feasibility of the autonomous sensor system. These results have motivated the desire to develop a similar system for powering up a LED either continuously as a light source or intermittently as a flashing indicator. However, a LED will not be possible to be lit up at observable luminosity if any of the transmitting devices is replaced by the LED in the above-mentioned autonomous system. This is because its power acquired is generally less than 20 mW and the LED requires power of 20 to 40 mW for normal operating [9].

This paper expands on the previous works described in [3-8] and investigates the capability of using the increasing number of identical piezoelectric benders (parallel and series configurations) for rising the power generation so that a self-powered system to flash a LED can be developed. Out of various ambient vibration sources, an air-conditioner (air-con) compressor can provides steadier and more continuous vibration for longer time and therefore it has been chosen in this paper for the system validation at the last stage. Benders (short cantilever beams) with polymeric piezoelectric element bonded on each of the bender were used for converting the vibration energy of such air-con compressor in operation into electrical energy. Due to the limited power harvesting with piezoelectric elements, the direct supply of energy for lighting a LED is not feasible. Therefore, the electric charge harvested from the piezoelectric elements was first accumulated until a sufficient amount before deliver to the LED. This results in discontinuous supply of energy to the LED and making LED to flash. The analytical models of series and parallel configurations of the given identical benders with its increasing number, n, were theoretically studied and experimentally compared to understand the performance of harvesting electric charge and power to flash a LED. After the validation of the self-powered system to flash a LED, this paper discuss the potential applications of (i) developing the flashing LED system into a module of self-powered decorative LED for the building or tree decorative light which consists of hundreds of this module; (ii) developing an autonomous sensor for monitoring the vibration amplitude of a vibrating object with the reference of LED flashing interval

2. Theoretical Study

2.1. Analytical Models for Piezoelectric Benders

A piezoelectric bender consists of a layer of polymeric piezoelectric element (its relative permitivity is 13) and a layer of host that they are bonded together. External stress to a piezoelectric bender in base vibration causes deflection and bending to the bender. The deflection distorts the internal dipole moments within the piezoelectric element and generates electrical voltages. This results in the generation of charges on the element. The relationship between the stress and strain of the piezoelectric element [10] are given as

$$\sigma_{piezo} = Y_{piezo}\left(\varepsilon_{piezo} - g_{31}D_3\right), \quad (1)$$

$$E_3 = -g_{31}\sigma_{piezo} + \frac{D_3}{13\varepsilon_0}, \quad (2)$$

where Y_{piezo} is the Young's Modulus of the polymeric piezoelectric element, ε_{piezo} and σ_{piezo} are the strain and stress of the element respectively in x direction, g_{31} is the piezo stress constant, D_3 and E_3 are electric displacement and electric field strength along the z direction, ε_0 is the permittivity of the vacuum, $\varepsilon_0 = 8.85\exp(-12)Fm^{-1}$.

For the equivalent mechanical model, the piezoelectric bender can be modeled as a single degree of freedom system (SDOF), which consists of a equivalent spring constant, *K*, of the piezoelectric beam, an equivalent mass, *M*, a dashpot with damping coefficient, *C*, and a vibrating base. The equivalent SDOF model is shown in Fig. 1, where *d(t)* is the vibrating base displacement and *x(t)* is the equivalent mass displacement. *y(t)* is the relative motion between the vibrating base and the equivalent mass, *M*. given by

$$y(t) = d(t) - x(t)\,. \quad (3)$$

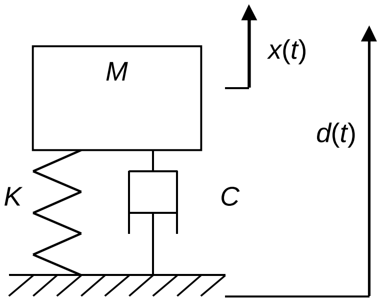

Fig.1. Equivalent SDOF model for the piezoelectric cantilever beam with excitation at base.

According to Newton's second law, the dynamic model of such system can be written as

$$M\ddot{y} + C\dot{y} + Ky = -M\ddot{d}\,. \quad (4)$$

Applying Laplace transform with zero initial conditions $y(0) = \dot{y}(0) = 0$, Eq. (4) becomes

$$y(s) = \frac{1}{s^2 + (4\pi f_0\xi)s + (2\pi f_0)^2}\ddot{d}(s), \quad (5)$$

where f_0 is the natural frequency and ξ is the damping ratio.

Assuming that the piezoelectric bender is excited at its base which is at the fixed end, the force $F(s)$ experienced by the beam because of the displacement input of y is given by

$$F(s) = Ky(s) = \frac{1}{s^2 + (4\pi f_0\xi)s + (2\pi f_0)^2}K\ddot{d}(s) \quad (6)$$

where K is the equivalent dynamic stiffness of the beam.

When a sinusoidal input $d(t) = d_0\sin(2\pi ft)$ is applied to the base excitation, Eq. (6) can be written as

$$F = Kd_0\sqrt{\frac{(2\xi r)^2 + 1}{(2\xi r)^2 + (1 - r^2)^2}}\sin(2\pi ft), \quad (7)$$

where $r = f/f_0$ is the ratio of the excitation frequency to the natural frequency.

The electric charge harvested on the piezoelectric element due to an external force, F, can be obtained by integrating the electric displacement to its overlapping area. The harvesting of electric charge for the piezoelectric bender can be obtained with the Eqs. (1) and (2), and expressed as

$$Q = \int_0^w \int_0^L D_3 dydx = \frac{13(1-A+AB)L^2\varepsilon_0}{kt_{bender}^{\;2}}\left[\frac{t_{bender}whV}{(1-A)L} - 3ABg_{31}F\right], \quad (8)$$

where

$$h = 1 + A^4(1-B)^2 - 2A(2A^2 - 3A + 2)(1-B) \quad (9)$$

$$k = h(1 - A + AB)\left(1 + 13Y_{piezo}\,g_{31}^{\;2}\varepsilon_0\right) - 39(1-A)A^2B^2Y_{piezo}\,g_{31}^{\;2}\varepsilon_0, \quad (10)$$

$$A = \frac{t_{host}}{t_{bender}}, \quad (11)$$

is the ratio of the host thickness, t_{host}, to the respective bender thickness, t_{bender},

$$B = \frac{Y_{host}}{Y_{piezo}}, \quad (12)$$

is the ratio of the Young's Modulus of the host, Y_{host}, to the Young's Modulus of the polymeric piezoelectric element, Y_{piezo}, V is the external applied voltage to the piezoelectric element, L and w are the length and width of the piezoelectric bender, respectively.

When the piezoelectric bender is used to harvest electric energy, there is no external applied voltage to the piezoelectric element attached ($V = 0$). As a result, the electric charge harvested on the piezoelectric element from Eq. (8) becomes

$$Q = \frac{-39AB(1-A+AB)g_{31}\varepsilon_0 L^2F}{t_{bender}^{\;2}k}. \quad (13)$$

Under converse piezoelectric effect, a piezoelectric element work as a sensor which is converting the mechanical energy into electrical signal and this element is modeled as an equivalent circuit which consists of a series capacitance, C, with a voltage source [11] (refer to Fig. 2). Since the piezoelectric energy harvester has the same working principle as the piezoelectric sensor, the same model is used in this paper for power harvesting application. One of the important parameters to be considered in both models is the capacitance of the piezoelectric material. This can be determined by first setting the external force, F, in Eq. (8) to zero which gives

$$Q = \frac{13(1-A+AB)L^2\varepsilon_0}{kt_{bender}^{\;2}}\left[\frac{t_{bender}whV}{(1-A)L}\right]. \quad (14)$$

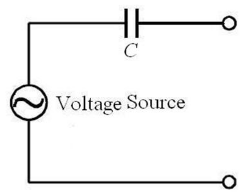

Fig. 2. Equivalent circuit of piezoelectric element.

Rearranging Eq. (14) give the capacitance as

$$C = \frac{Q}{V} = \frac{13(1-A+AB)hwL\,\varepsilon_0}{(1-A)t_{bender}\,k}. \quad (15)$$

In order to increase the power transferred to the LED, more than one piezoelectric bender could be used to raise the harvested power. When more than one bender are used, these benders can be connected in various combinations (i.e. parallel only, series only and any mixture of parallel and series). With the understanding of combining capacitance in electricity study, their electric charge generated and effective piezoelectric capacitance can be determined. Since the parallel only combination possesses maximum electric charge harvested and effective capacitance and the series only combination possesses minimum electric charge generation and effective capacitance among all the possible combinations, only these two extreme combinations are considered in this study. When n identical piezoelectric benders are used, their electric charge harvested and effective piezoelectric capacitance for the two combinations (n-parallel and n-series configurations) become

$$Q_{n-parallel} = \frac{-39nAB(1-A+AB)g_{31}\varepsilon_0 L^2F}{t_{bender}^{\;2}k}, \quad (16)$$

$$Q_{n-series} = \frac{-39AB(1-A+AB)g_{31}\varepsilon_0 L^2F}{t_{bender}^{\;2}k}, \quad (17)$$

$$C_{n-parallel} = \frac{13n(1-A+AB)hwL\,\varepsilon_0}{(1-A)t_{bender}\,k}, \quad (18)$$

$$C_{n-series} = \frac{13(1-A+AB)hwL\,\varepsilon_0}{n(1-A)t_{bender}\,k}. \quad (19)$$

Therefore, for *n*-parallel configuration, the electric charge harvested is in direct proportion to the applied forces and the number of the identical benders, *n* (Eq. (16)), whereas, the effective piezoelectric capacitance is directly proportional to *n* (Eq. (18)).

For *n*-series configuration, the electric charge harvested is independent on *n* but it is still in direct proportion to the applied forces (Eq. (17)), but the effective piezoelectric capacitance is inversely proportional to *n* (Eq. (19)).

2.2. Power Harvesting Circuit and Energy Conversion

The block diagram of the proposed power harvesting circuit is shown in Fig. 3. In order to be able to light up the LED, electric current in the LED has to be large enough. A DC – DC buck converter approach is deployed to amplify the current by reducing the voltage output [12]. To achieve higher current in LED, the duty cycle is incrementally increased or decreased by a control circuit to change the current level on the current versus duty cycle curve. With the designed algorithm [13], the adaptive controller is used to manage the maximum power into the LED.

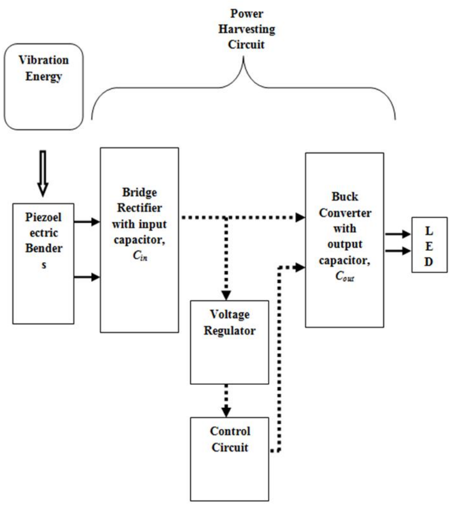

Fig. 3. Block diagram of piezoelectric energy power harvesting circuit.

Since piezoelectric elements produce AC voltage under vibration and LED needs a DC current, the piezoelectric energy is first rectified then used to charge up an input capacitor. When the input capacitor is charged to a predetermined value, $V_{in} = V_{max}$, it will discharge into the buck converter and this voltage is monitored by the control circuit. When the input to the buck converter falls below a required level, $V_{in} = V_{min}$, the control circuit turns off the discharge process so that the capacitor is allowed to charge up again.

By considering the piezoelectric capacitor (Fig. 2) and the input capacitor (Fig. 3) of the harvesting circuit are connected in series and assuming the rectifier is ideal, the average piezoelectric power harvested, P_{piezo}, is given as

$$P_{piezo} = 2fW_{piezo} = 2f\left[\frac{1}{2}\left(\frac{Q_{tot}^{2}}{C_{tot}}\right)\right] = \frac{fQ_{tot}^{2}}{C_{tot}} \quad (20)$$

where W_{piezo} is the electric energy harvested per bending, Q_{tot} is the total electric charge harvested, C_{tot} is the combined capacitance of piezoelectric capacitance and f is the frequency of the vibration experienced by the piezoelectric elements.

The electric energy transferred, $W_{transfer}$, into the rectifier circuit during one discharging process can be determined by using

$$W_{transfer} = \frac{1}{2}C_{in}\left(V_{\max}^{2} - V_{\min}^{2}\right). \quad (21)$$

where C_{in} is the input capacitance.

Thus, the average electric power transferred into the rectifier circuit can be expressed as

$$P_{transfer} = \frac{W_{transfer}}{\tau}, \quad (22)$$

where τ is the charging and discharging time of the input capacitor.

And the efficiency of power transferred from the piezoelectric elements during vibration into the rectifier circuit is written as

$$\eta_{power} = \left(\frac{P_{transfer}}{P_{piezo}}\right)100\%. \quad (23)$$

3. Experiment and Results

The piezoelectric elements used in the experiment are the 52 μm piezo film from Measurement Specialties, Inc. and the host material is polypropylene. The piezo stress constant, g_{31}, is given as 216 x 10^{-3} m^2C^{-1}. The length and width of each piezoelectric bender are 125 *mm* X 11 *mm*, respectively. As a result, *A* (Eq. (11)) and *B* (Eq. (12))are 0.704 and 0.3, respectively. With this configuration, the piezoelectric bender will have its resonance frequency at 20 *Hz*.

In order to ease the comparison between the results of the laboratory experiment and that of real application testing in the later section, the vibration frequency, *f*, and the external force, *F*, applied using the shaker to the base of the benders are set to be 20 *Hz* and 2.3 *mN*, respectively, in the experiment. These values are the typical vibration frequency and the input force from the vibrating air-con compressor when the fan speed is at 1200 *rpm* (refer to section 4 for the prototype performance analysis for comparison).

For verifying the theoretical electric charge harvesting in this paper, the experiment was first setup without the converter and LED (refer to Fig. 4). The input capacitance used is C_{in} = 23 μF and its voltage is V_{in}. The maximum value of V_{in} is $V_{in,\max}$, and the charging time for the input capacitor from V_{in} = 0 to $V_{in,\max}$ is *t*. The experiment was conducted for both the parallel and the series configurations with *n* = 1 to 10. Each set of $V_{in,\max}$ and *t* were measured. In experiment, a bridge rectifier with four schottky barrier diodes was used in order to ensure the low loss of energy transfer from the piezoelectric elements to the converter. By assuming the rectifier is ideal and ignoring the existence of the rectifier (refer to Fig. 5), the input capacitor is considered to be in series with the piezoelectric capacitor and, thus, the piezoelectric capacitor has the same amount of electric charge as the input capacitance. The electric charge harvested per bending in experiment, $Q_{\exp}$, can be determined by

$$Q_{\exp} = \frac{C_{in} V_{in,\max}}{2 ft}, \tag{24}$$

where C_{in} and $V_{in,\max}$ were the measured values.

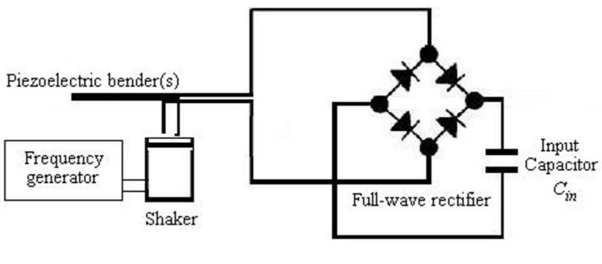

Fig. 4. Experiment setup for determination of electric charge harvesting.

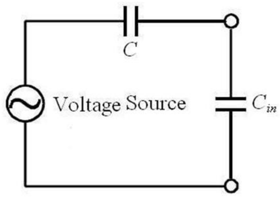

Fig. 5. Equivalent circuit of Fig. 3 by ignoring the rectifier bridge.

The comparison of the experiment and the simulation (using Eqs. (16) and (17)) shows that the experimental electric charge harvested is in good agreement with the theoretical prediction. This is clearly shown in Fig. 6. The electric charge harvested increases directly proportional to *n*, in the *n*-parallel configuration and that is independent on *n* in the *n*-series configuration.

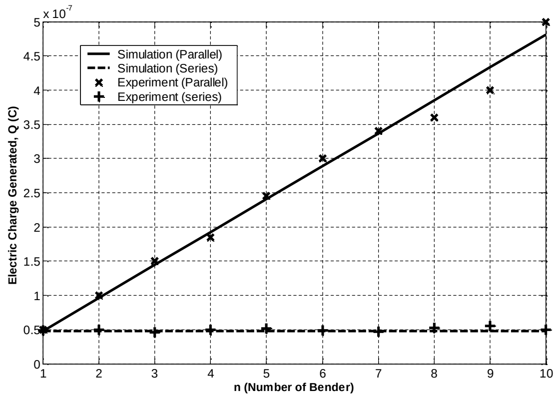

Fig. 6. Results of simulation and experiment for electric charge harvesting.

For verifying the theoretical effective piezoelectric capacitance, a digital capacitance meter was then used to measure the effective piezoelectric capacitance and the theoretical simulation is based on Eqs. (18) and (19). Fig. 7 shows the results of both the simulation and the measurement. The measurement seems to agree very well with theoretical simulation. The analytical Eqs. (18) and (19) for the effective piezoelectric capacitance for both the parallel and the series configurations up to *n* = 10 are, therefore, verified.

During the experiment with a LED from HB Electronic Components [14] loaded to the converter (Fig. 3), the voltage of the input capacitor (C_{in} = 24 μF), V_{in}, was found to reach 4.95 *V* (V_{max}), and then it discharged into the converter circuit until V_{in} falls below 3.93 *V* (V_{min}) as shown in Fig. 8. The discharging process was

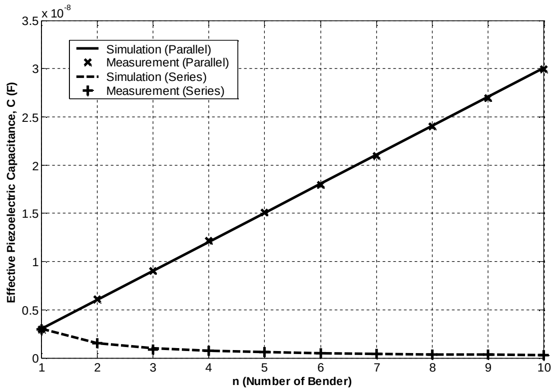

Fig. 7. Results of simulation and measurement of piezoelectric capacitance.

terminated by the control circuit so that the input capacitor could be charged up again. Since the values of V_{max} (4.95 V) and V_{min} (3.93 V) in this experiment were predetermined at the circuit design, the change in $V_{in} = V_{max} - V_{min}$ is a constant. However, the rate of the change in V_{in} was affected by the parameters of n and the configuration of the benders. Fig. 8 shows the change in V_{in} with time for n = 5 in parallel configuration for example. Using Eq. (21), $W_{transfer}$ was found to be 108.7 μJ per change in voltage in this experiment.

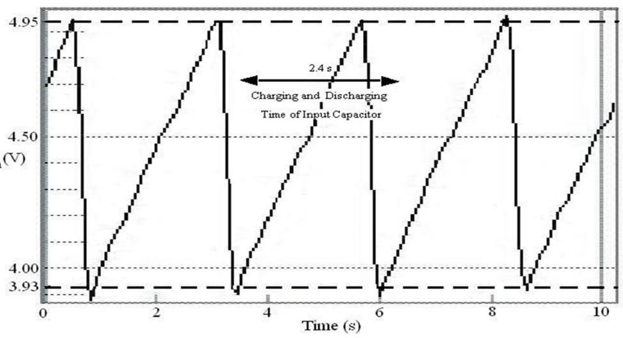

Fig. 8. Change in V_{in} with time for n = 5 in parallel configuration.

One of the important information to be considered in this experiment is the efficiency of the converter which can be determined as follows. The electrical energy transferred from the input capacitor into the converter is first stored in the output capacitor, C_{out} (refer to Fig. 3), which is later channeled into the LED. In this experiment, C_{out} = 82.7 μF and the range of voltage of output capacitor, V_{out}, was found to change from 1.5 V to 1.25 V (Fig. 9). Similar to V_{in}, the change in V_{out} remains constant as long as the same LED loaded. The result shows that the electric energy of 28.5 μJ has transferred to the LED during one cycle of charging and discharging of the output capacitor. Since the energy input to rectifier circuit and that output to the converter circuit acquired are 108.7 μJ ($W_{transfer,input}$) and 28.5 μJ ($W_{transfer,output}$), respectively, the efficiency of the converter in this experiment is 26.6%.

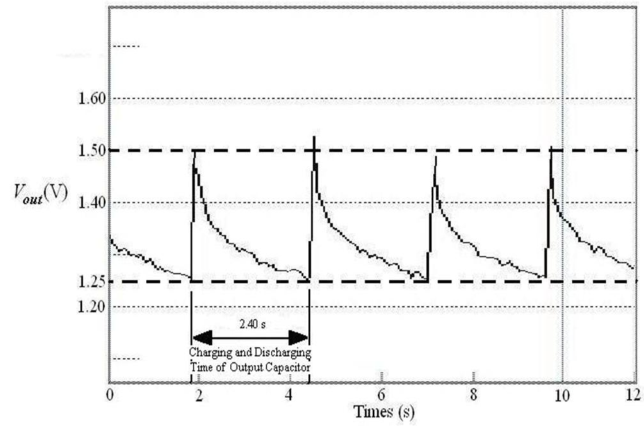

Fig. 9. Change in voltage of the output capacitor for n = 5 in parallel configuration.

The performance of the piezoelectric benders as a power generator can be determined by measuring the duration of a charging and discharging cycle in the output capacitor was conducted for each of the configurations with n up to 10. This result (refer to Fig. 10) shows that the duration decreases as n increases for both the parallel and series configurations. However, the parallel configuration has shorter duration than that in the series configuration. Due to the rapid discharge of the capacitor through the LED, a short burst of large enough electric current is produced and hence causes the LED to flash. This duration of the cycle is, therefore, referred as the flashing interval of the loaded LED. Thus, the results shown in Fig.10 can be referred as the flashing intervals of the LED for piezoelectric benders in parallel and series configurations. The shortest flashing interval of the LED was 1.15 s with n = 10 in parallel configuration. Shorter flashing interval means more electric charge and power are harvested so that the LED can be flashed more rapidly. Fig. 11 shows the ratio of the flashing interval with series configuration to parallel configuration for n = 1 to 10 obtained through experiment. It was found that the ratio increases with n. This means that the flashing interval with parallel configuration is smaller than that with series configuration. However, as the curve gradient (Fig. 11) reduces as *n* increases, the decrement in the flashing interval with parallel configuration reduces for increasing *n*. Since flashing interval with parallel configuration is generally shorter than that with series configuration, the piezoelectric benders in parallel configuration is concluded to perform better electric charge generation and power harvesting to flash the LED and the performance can be improved further with increasing *n*.

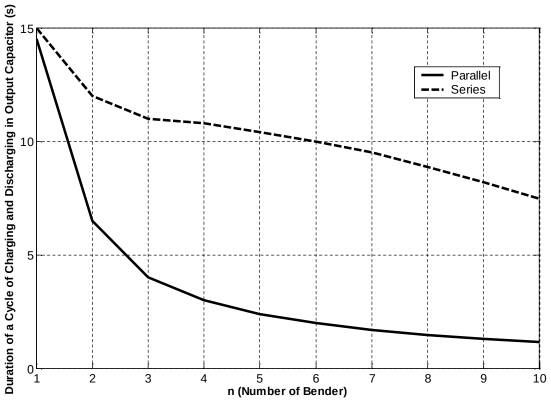

Fig. 10. Duration of a charging and discharging cycle in the output capacitor.

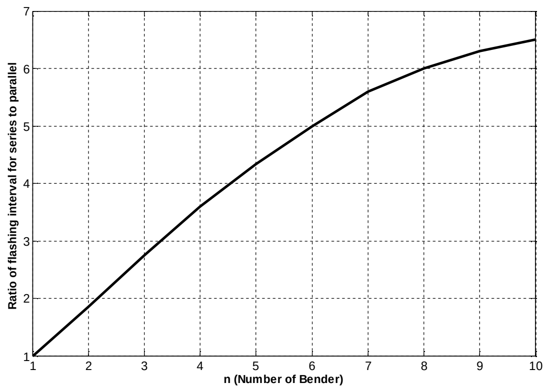

Fig. 11. Ratio of flashing interval with configurations of series to parallel for *n* = 1 to 10.

With reference to the experimental results of electric charge generated and the effective piezoelectric capacitance (Fig. 6 and Fig. 7), the average piezoelectric power harvested and the average power transferred to the rectifier circuit were calculated using Eqs. (20) and (22), respectively. The average power transferred to the converter circuit, $P'_{transfer}$, was determined by

$$P'_{transfer} = \frac{\frac{1}{2}C_{out}\left(V'^{\,2}_{\max} - V'^{\,2}_{\min}\right)}{\tau}, \qquad (25)$$

where V'_{max} = 1.5 *V* and V'_{min} = 1.25 *V* in this experiment.

Fig. 12 shows the results of the average piezoelectric powers harvested and the average power transfer with parallel and series configurations as a function of benders number, *n*. The average piezoelectric power harvested with parallel configuration was found to be coincided with that of series configuration. This means that the average power harvested for a given *n* is independent to the configuration. However, the average power transfer for parallel configuration was observed to be always larger than that for series configuration due to the fact of larger electric charge harvested per bending of the piezoelectric elements in parallel configuration. The average power transfer to the converter circuit was less than that to the rectifier circuit, as expected, due to power lost and impedance mismatch between the circuits. By using Eq. (23), the efficiency of each of the average power transfer to the rectifier circuit and that to the converter circuit was obtained which is shown in Fig. 13. It was observed that the transfer efficiency in parallel configuration increases as *n* increases. This is because this configuration provides better match in the source impedance to the input impedance in the rectifier circuit. The converter circuit was found to have constant transfer efficiency at 26.2% always. Fig. 14 outlines the power flow and system characteristics of five piezoelectric benders in parallel configuration.

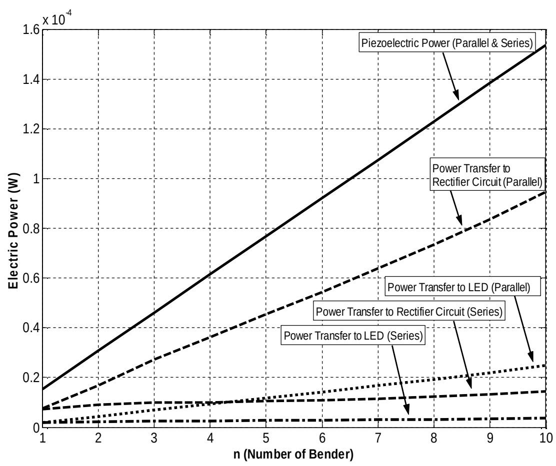

Fig. 12. Piezoelectric power and power transfer for parallel and series configurations.

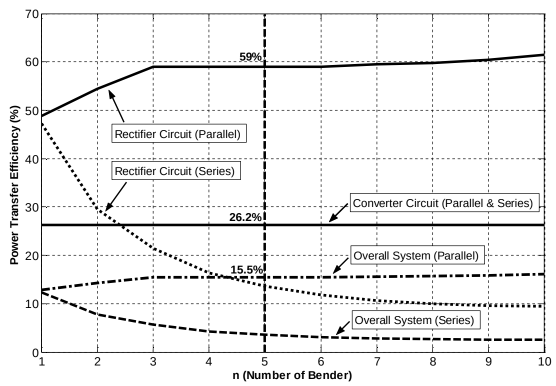

Fig. 13. Experimental power transfer efficiencies for parallel and series configurations.

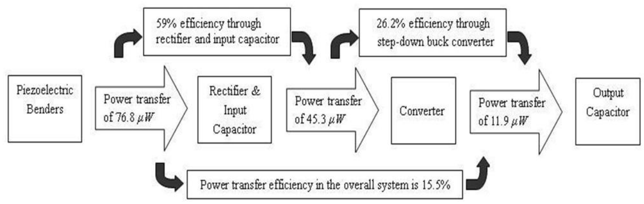

Fig. 14. Outline of power flow and system characteristics.

In order to estimate the average power for flashing the LED used in experiment, the intensity of the emitted light from the LED was measured. It can be seen from Fig. 15 that the LED flashing interval was 2.4 *s* and the duration for the LED emitting light was approximate 1.8 *s* when five piezoelectric benders in parallel configuration were used. Other than these, the highest light intensity reached and its average were found to be about 3 *Lux* and 0.35 *Lux*, respectively. By referring to the LED characteristics graphs as shown in Fig. 16, for the average light intensity of 0.35 *Lux*, the equivalent forward current, *I*, and voltage, *V*, were acquired to be 7.5 *mA* and 3.0 *V*, respectively. Hence, the average power for flashing the LED is estimated as 22.5 *mW*.

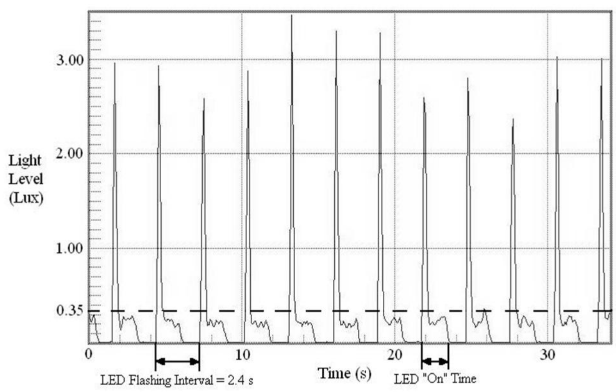

Fig. 15. Light intensity emitted by the flashing LED.

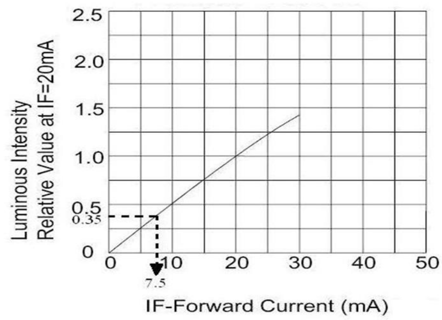

(a)

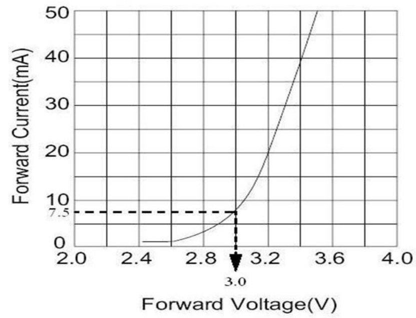

(b)

Fig. 16. Characteristics graphs of the LED used in experiment. [14] (a) Light intensity Vs Forward current; (b) Forward current Vs Forward voltage.

4. Test on the Piezoelectriv Energy Harvester Prototype

The piezoelectric benders in parallel configuration and the power harvesting circuit discussed above form a prototype of the piezoelectric energy harvester. This prototype was tested its workability as a self-powered light indicator for the two potential applications by placing it on the casing of a selected air-con compressor (refer to Fig. 17). The typical fan speeds in this compressor are about 700 *rpm*, 900 *rpm* and 1200 *rpm*. These provide the fundamental mode of vibration in the frequencies of 11.7 *Hz*, 15 *Hz* and 20 *Hz*. By using *n* = 1 to 10, the results of the prototype testing with the three different vibration frequencies were obtained. Fig. 18 shows the comparison of the test results with the experimental results. The shortest LED flashing interval was found to be 1.50 *s* at 20 *Hz* when *n* = 10 .This is because when the compressor fan turned 1200 *rpm* (20 *Hz*), the piezoelectric benders were in resonance. Thus, more electric charge was harvested and resulted in the highest LED flashing rate. The test results of the rate of LED flashing is consistent with the experimental results for *n* = 1 to 10 under the same vibrating frequency. However, due to the existence of additional mechanical damping in the test structure, the overall test results were observed to be approximate 30% difference from the experimental results.

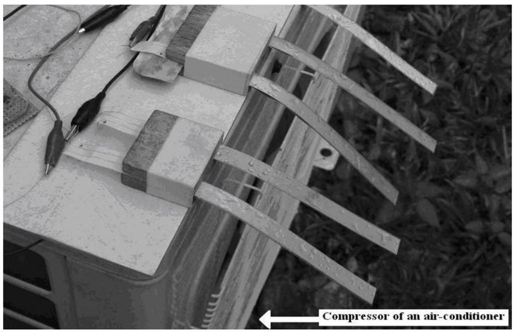

Fig. 17. Piezoelectric energy harvester prototype placed on the air-con compressor.

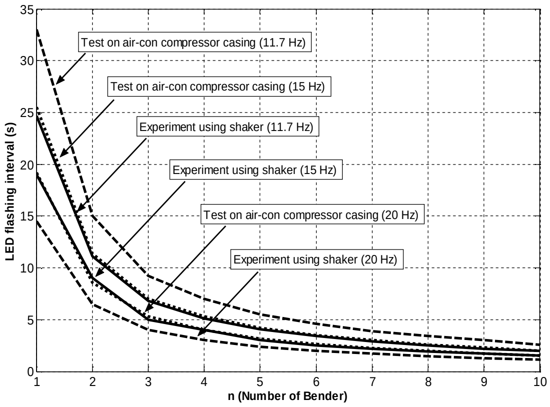

Fig. 18. Comparison between the results of experiment and prototype testing.

In view of the LED flashing intervals (2.6 *s*, 2.0 *s*, 1.5 *s* for 11.7 *Hz*, 15 *Hz*, 20 *Hz*, respectively) in the test results when n = 10, the workability as a self-powered light indicator (Fig. 19) for the two mentioned applications is therefore validated within the consideration of the mechanical damping of the vibrating structure.

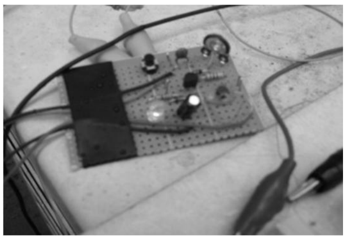

Fig. 19. Power harvesting circuit prototype with the flashing LED.

5. Conclusions

In this paper, the analytical models of series and parallel configurations of the given identical piezoelectric benders with increasing bender number, n, were established. From the results of the experiment, the electric charge harvesting with the benders in parallel configuration is n times of the charge harvesting in series configuration since the charge generation in series configuration is always constant. The piezoelectric benders in parallel configuration were found to perform the best and the electric charge and power harvested were increased with increasing n. By using shaker to provide steady and continuous vibration to the benders, the LED flashing interval for the benders in parallel configuration is 1.15 *s* at n = 10. The recorded LED flashing light intensity was estimated to be 22.5 *mW*. By placing on the casing of an air-con compressor for testing its workability as a module of self-powered decorative LED as well as an autonomous monitoring system for shaking amplitude of the compressor casing at a particular fan speed with reference to the LED flashing interval, the test results of the rate of LED flashing is consistent with the experimental results for n = 1 to 10 under the same vibrating frequency. Hence, the workability of the suggested applications is validated within the consideration of the structural damping.

Acknowledgements

This study was supported by the Malaysian Ministry of Science, Technology and Innovation (MOSTI) under e-Sciencefund 03-01-10-SF0144, and is greatly acknowledged.

References

[1] T. Starner, "Human-powered Wearable Computing", IBM Systems J., vol. 35(3 & 4), pp. 618-629, 1996.

[2] N.S. Shenck, and J.A. Paradiso, "Energy Scavenging with Shoe-Mounted Piezoelectrics", J. IEEE Micro, vol. 21(3), pp. 30 – 42, 2001.

[3] J. Kymissis, C. Kendall, J. Paradiso, and N. Gershenfeld, "Parasitic power harvesting in shoes", Proc. 2nd IEEE ISWC, pp. 132-139, 1998.

[4] T.H. Ng, and W.H. Liao, "Sensitivity Analysis and Energy Harvesting for a Self-Powered Piezoelectric Sensor", J. of Int. Material Systems & Structures, vol. 16, pp. 785-797, 2005.

[5] E. Lefeuvre, A. Badel, C. Richard, and D. Guyomar, "Piezoelectric Energy Harvesting Device Optimization by

Synchronous Electric Charge Extraction”, J. of Int. Material Systems & Structures, vol. 16, pp. 865 – 876, 2005.

[6] Y.K. Tan, K.Y. Hoe, and S.K. Panda, “Energy Harvesting using Piezoelectric Igniter for Self-Powered Radio Frequency (RF) Wireless Sensors”, Proc. of IEEE ICIT, Mumbai, India, pp. 1711–1716, 2006

[7] Y.K. Tan, J.Y. Lee, and S.K. Panda, “Maximize Piezoelectric Energy Harvesting Using Synchronous Charge Extraction Technique For Powering Autonomous Wireless Transmitter”, Proc. of IEEE ICSET, Singapore, pp. 1123-1128, 2008.

[8] Yee Win Shwe, and Yung C. Liang, “Smart Dust Sensor Network with Piezoelectric Energy Harvesting”, Proc. 6th ICITA, 2009.

[9] LEDtronics Discrete LED Color Chart, LEDtronics, Inc.23105 Kashiwa Ct, Torrance, CA 90505 – PH.

[10] J.P. Ayers, D.W. Greve, and I.J. Oppenheim, “Energy Scavenging for Sensor Applications Using Structural Strains”. SPIE, vol. 5057, pp. 364-375, 2003.

[11] J. Karki, Signal Conditioning Piezoelectric Sensors, App. Rept. on Mixed Signal Products (SLOA033A), Texas Instruments Incorporated, 2000.

[12] H.Maruta, F.Kurokawa, J.Sakemi, A.Nakamura, and H.Osuga, “A New Prediction Based Digital Control for DC-DC Converter”. International Journal Of Renewable Energy Research , IJRER vol.1, no.2, pp.76-85, 2011.

[13] S.Belfedhal, and E.Berkouk, “Modeling and Control of Wind Power Conversion System with a Flywheel Energy Storage System”. International Journal Of Renewable Energy Research , IJRER vol.1, no.3, pp.152-161, 2011.

[14] LED Specification, Part No.: 530xW 8C, HB Electronic Components.